Chipping Detection in Ceramic Insert during Turning by Analysis of Workpiece Surface Profile Using Cross-Correlation

IOP Conf. Series: Materials Science and Engineering **530** (2019) 012007 doi:10.1088/1757-899X/530/1/012007

Chipping Detection in Ceramic Insert during Turning by Analysis of Workpiece Surface Profile Using Cross-Correlation

N A Mohamad and M M Ratnam*

School of Mechanical Engineering, Engineering Campus, Universiti Sains Malaysia, 14300 Nibong Tebal, Penang, Malaysia.

Corresponding author *: mmaran@usm.my

Abstract. Chipping in ceramic cutting inserts during machining can cause detrimental effects on the surface finish quality of the workpiece. Current methods of detecting chipping in ceramic inserts do not compare the minute changes in the workpiece profile in subsequent machining passes. In this work, an effective method of detecting chipping in ceramic inserts by analysing the workpiece surface profile using cross-correlation is proposed. In this method, the sub-pixel edge location method was used to extract the surface profile captured using a digital camera. Surface profiles corresponding to subsequent machining passes were cross-correlated at three different sections of the workpiece. An abrupt drop in the correlation coefficient was observed in the middle and end sections of the workpiece after the fifth machining pass, thus providing a reliable measure of tool chipping.

1. Introduction

Ceramic cutting tool inserts are the preferred type of cutting tools for the machining of hard and difficult-to-cut materials such as alloy steels. This is due to their high hot hardness and wear resistance. However, due to their inherent low toughness ceramic inserts have be reported to undergo ladder-like chipping, cracking and fracture during machining [1-3]. Since failure of a cutting tool during machining will cause a detrimental effect on the finished product, the early detection of wear in the cutting tool is an important area of research. Although a significant amount of research has been published on the offline and in-process detection of wear in cutting tools [4-7], most of these researches are limited to carbide tools. The detection of wear and chipping in ceramic cuttings inserts has been investigated only by a few researchers.

Neslušan et al. [8] developed a method to detect the breakage of ceramic cutting tools during hard turning by analyzing acoustic emission (AE) signals. AE signals are known to be sensitive to the plastic deformation processes linked with dislocation slips during machining of ductile materials or brittle cracking. The authors used two AE sensors with different frequency ranges to detect machining changes before and after tool breakage. This method, however, is not sensitive to detect the occurrence of chipping in the ceramic tool. Lee at al. [9] used fast Fourier transform (FFT) to detect the onset of chipping in commercial ceramic cutting inserts. The edge profile of the workpiece was extracted to sub-pixel accuracy and the extracted profile was transformed from the spatial domain to the frequency domain using FFT. During gradual wear the amplitude of the fundamental feed frequency was observed to increase steadily, but after the onset of tool chipping significant fluctuations in the feed frequency was observed. Although this method was shown to be effective in detecting the onset of chipping the edge profiles before and after chipping were not compared quantitatively. In a later publication [10], the

authors applied the sub-window FFT and continuous wavelet transform (CWT) methods to detect the onset of chipping in ceramic tools. They reported that compared to the sub-window FFT method the CWT method is more effective in detecting the exact onset of tool chipping. The authors also investigated the effectiveness of the autocorrelation method in detecting chipping in ceramic inserts by analyzing the workpiece profile captured using a digital camera [11]. The authors reported that chipping in the tool caused the peaks of the autocorrelation function to decrease rapidly with increase in lag distance. The correlation was made between profiles recorded from the same section of the workpiece but at different angles. The profiles at various parts of the workpiece were not cross-correlated to detect chipping in the tool.

Besides the work done by Lee et al. [9-11] there is very little published literature on the detection of chipping in ceramic cutting tools. Many researchers have reported the problem of chipping in ceramic cutting inserts but a reliable method of detecting chipping is yet to be developed. The aim of this paper is to propose a vision-based method combined with sub-pixel edge location and cross-correlation to detect the occurrence of chipping in commercial cutting tools during dry turning.

2. Methodology

2.1. Experimental setup and image capture

The dry turning operation was conducted by using a 45 mm diameter AISI 305 stainless steel workpiece of length 200 mm. The machining was done on a *Pinocho S90* conventional lathe machine by using ceramic insert cutting tool from Sandvik Coromant Ltd., Sweden. The workpiece was mounted securely at both ends to ensure there is minimum vibration during turning (Figure 1(a)). The machining was carried out using a cutting speed of 1400 rpm, feed rate of 0.3 mm/rev and a depth-of-cut of 1 mm. A high cutting speed and feed rate were used to accelerate the rate of wear in the ceramic insert. The machining was done for five passes. After each pass the workpiece was removed from the lathe to capture the profile. The cutting tool insert was also removed and observed under that scanning electron microscope. The machined length was divided into three sections, namely start, middle and end, for the surface analysis (Figure 1(b)). A high-resolution DSLR camera (pixel resolution: 5184 × 3456 pixels) fitted with a macro lens was used to capture the edge profile of the machined workpiece with the aid of backlighting (Figure 1(c)). The intensity of the backlighting was controlled appropriately to ensure the image is not too bright or too dark. The surface of the workpiece was cleaned using a jet to compressed air before capturing the images. The workpiece was shifted using a translation stage in order to capture images at various sections. Four images were captured at each section by rotating the workpiece by 90°.

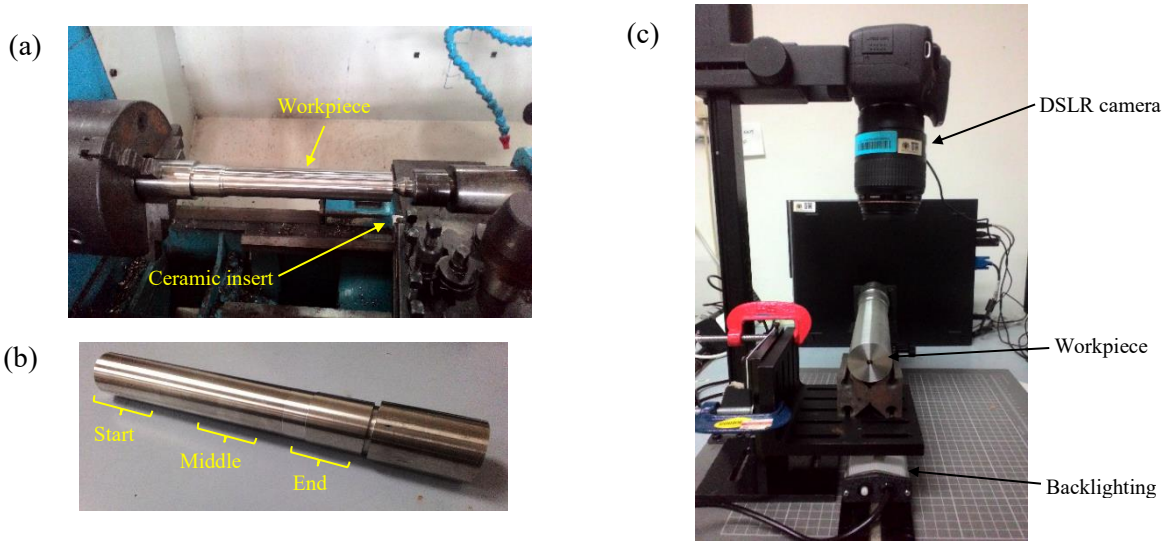

Figure 1. (a) Machining setup, (b) various section used in analysis, (c) setup for capturing workpiece profile.

2.2. Profile extraction using sub-pixel edge location

Figures 2(a) shows the sample raw image of the workpiece profile captured after the first pass. The profile of the workpiece surface was extracted using the invariant-moment sub-pixel edge detection method originally proposed by Tabatabai and Mitchell [12]. In this method a scan line across a step edge is characterized by a set of numbers x_i, where i= 1, 2, 3, …, n. The edge is defined between a sequence of pixels at one intensity level h_1 followed by a sequence pixels at another intensity level h_2 as illustrated in Figure 2(b). The first three moments m_1, m_2 and m_3 of the input data sequence are given by a threshold independent method based on grey level moment equations, whereby the moments are defined as a sum of the pixel intensity powers. The i^{th} moment of the input grey level data sequence x_j is given by

$$\bar{m}_i = \frac{1}{n}\sum_{j=1}^{n}(x_j)^i \tag{1}$$

where x_1, x_2,…, x_n are pixel intensities and n is the total number of pixels in row j. If k denotes the number of h_1 values in the ideal edge, then the first three samples moments between input and output sequences can be solved in three equations by:

$$\bar{m}_i = \sum_{j=1}^{2} p_j h_j^i \tag{2}$$

where i = 1, 2 and 3, and p_h = number of pixels with grey intensity values h.

With the three unknowns h, k and p_2, the solutions of the edge are calculated by:

$$h_1 = \bar{m}_1 - \sigma\sqrt{\frac{p_2}{p_1}} \tag{3}$$

$$h_2 = \bar{m}_1 + \sigma\sqrt{\frac{p_1}{p_2}} \tag{4}$$

$$p_2 = \frac{1}{2}\left[1 + s\sqrt{\frac{1}{4+s^2}}\right] \tag{5}$$

$$p_1 = 1 - p_2 \tag{6}$$

where $\sigma = \sqrt{\bar{m}_2 - \bar{m}_1^2}$ and s defined as the skewness of the input data sequence given by,

$$s = \frac{2\bar{m}_1 + \bar{m}_3 - 3\bar{m}_1\bar{m}_2}{\sigma^3} \tag{7}$$

Thus, the edge location of the workpiece up to sub-pixel accuracy is determined by:

$$k = p_1 n \tag{8}$$

The invariant moment method of sub-pixel edge detection allows precise edge location as shown by the red line in Figure 2(c).

2.3. Simulation analysis using cross-correlation

Cross-correlation is essentially a measure of similarity between two signals as a function of displacement of one relative to the other. For two continuous function $f(t)$ and $g(t)$ the cross-correlation is given by the dot product,

$$f * g = \int_{-\infty}^{\infty} f^*(t) g(t + \tau) dt \tag{9}$$

where f^* is the complex conjugate of f and τ is the displacement, also known as the lag distance. For discrete function such as the digitized surface profile, the cross-correlation is defined as,

$$f * g = \sum_{n=-\infty}^{\infty} f^*(k) g(k + l) \tag{10}$$

where k is a measure along the signal length and l is the lag distance.

(a)

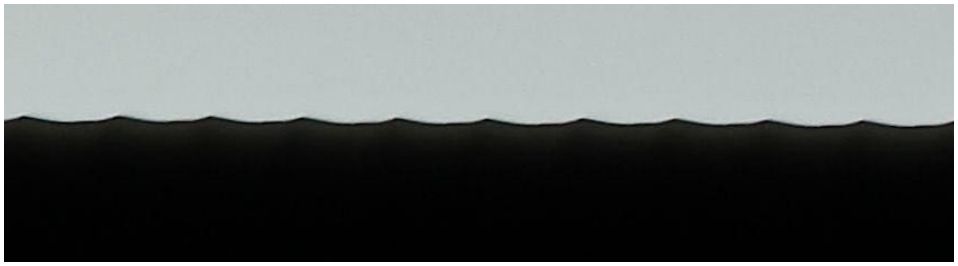

(b)

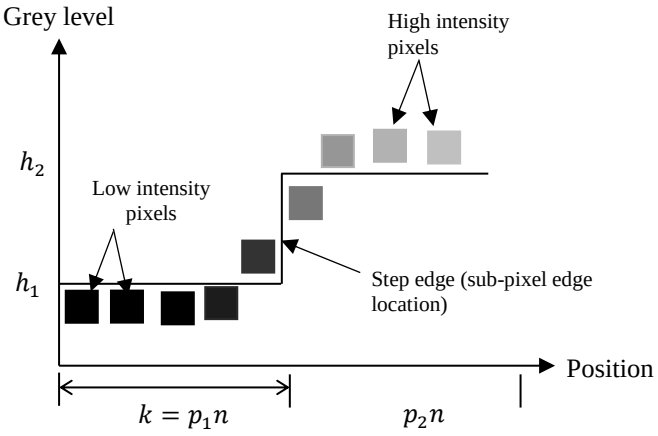

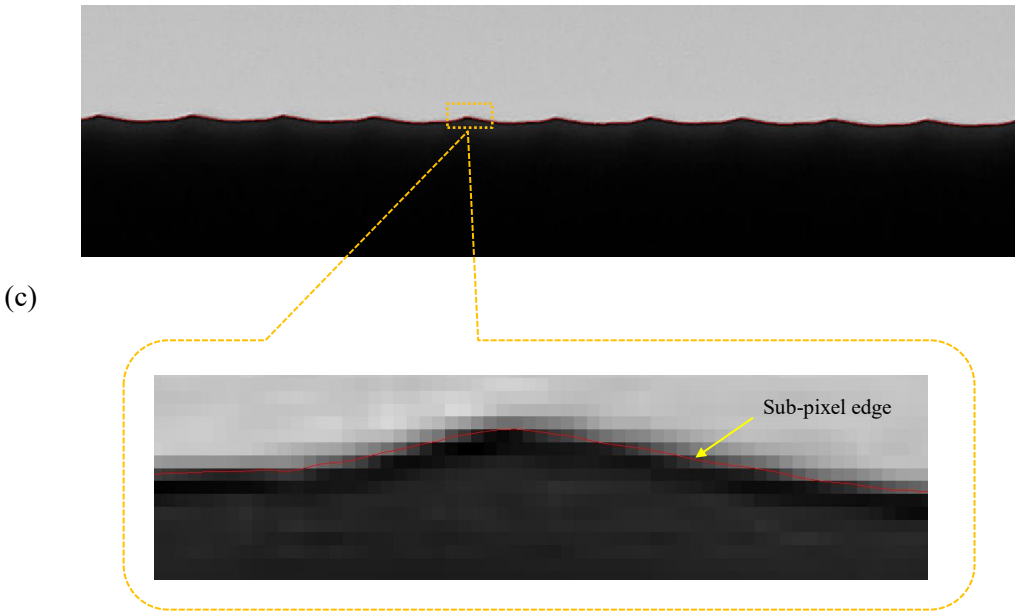

Figure 2. Extraction of workpiece edge profile to sub-pixel level: (a) raw image, (b) grey value variation in the invariant moment method, (c) extracted profile (shown in red).

Figures 3(a)-(c) show three simulated profile, whereby Figure 3(a) is assumed to be shaped by a new cutting tool, Figure 3(b) is formed by a slightly worn cutting insert while Figure 3(c) is formed by a badly worn cutting insert. The corresponding extracted profiles are shown in Figures 4(a)-(c).

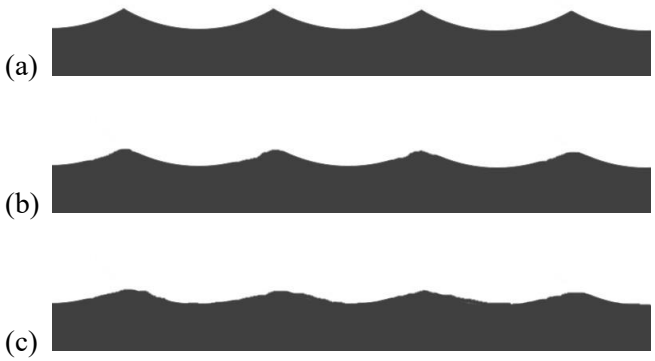

Figure 3. Simulated profiles: (a) formed by new insert, (b) formed by slightly worn inset, (c) formed by badly worn insert.

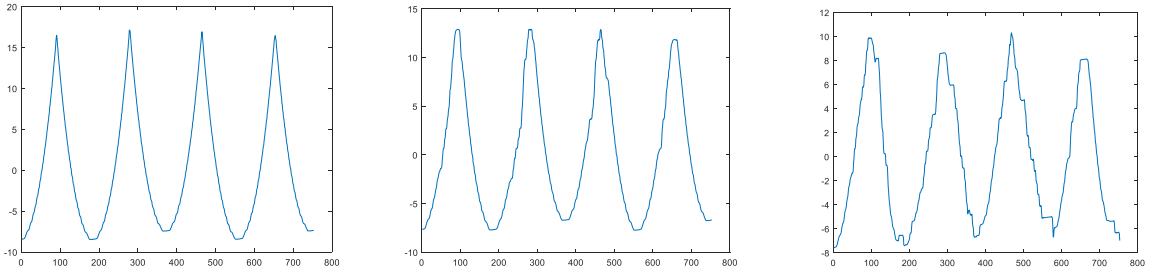

(a) (b) (c)

Figure 4. Extracted profiles corresponding to Figures 3(a)-(c).

The result of cross-correlating the profiles in Figure 4(a) with Figure 4(b) and Figure 4(a) with Figure 4(c) is shown in Figure 5(a) and 5(b). Although the correlation plots look the same the maximum correlation value when the insert is slightly worn is 0.9931 while the corresponding value when the insert is badly worn is 0.9539. The maximum positive correlation coefficient thus gives a measure of the wear condition of the insert.

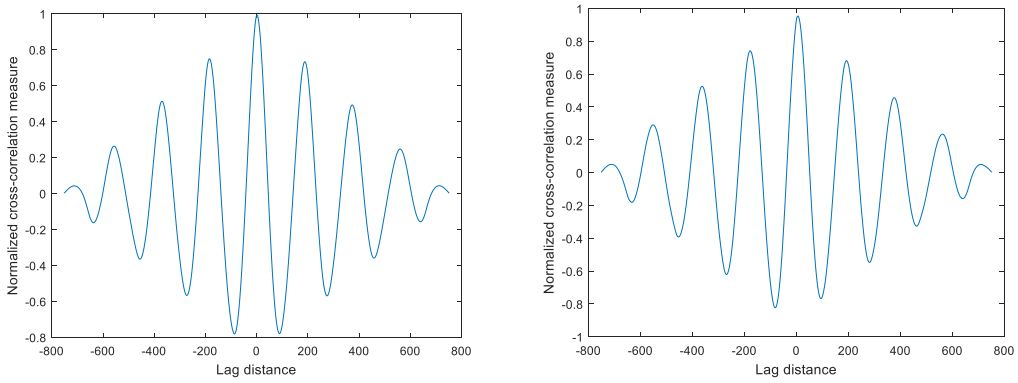

Figure 5. Plot of cross-correlation for (a) slightly worn insert, (b) badly worn insert.

3. Results and Discussion

Figures 6(a)-(e) show the workpiece edge profiles at various stages of machining and the insert image captured at the end of each pass. The gradual change in the profile during the first four passes is clearly noticeable while there is a rapid change in profile from the 4th to the 5th pass. The gradual profile change can be attributed to the gradual loss of tool material during turning while the rapid change in the profile is due to chipping (highlighted in yellow on the insert image).

(a)

(b)

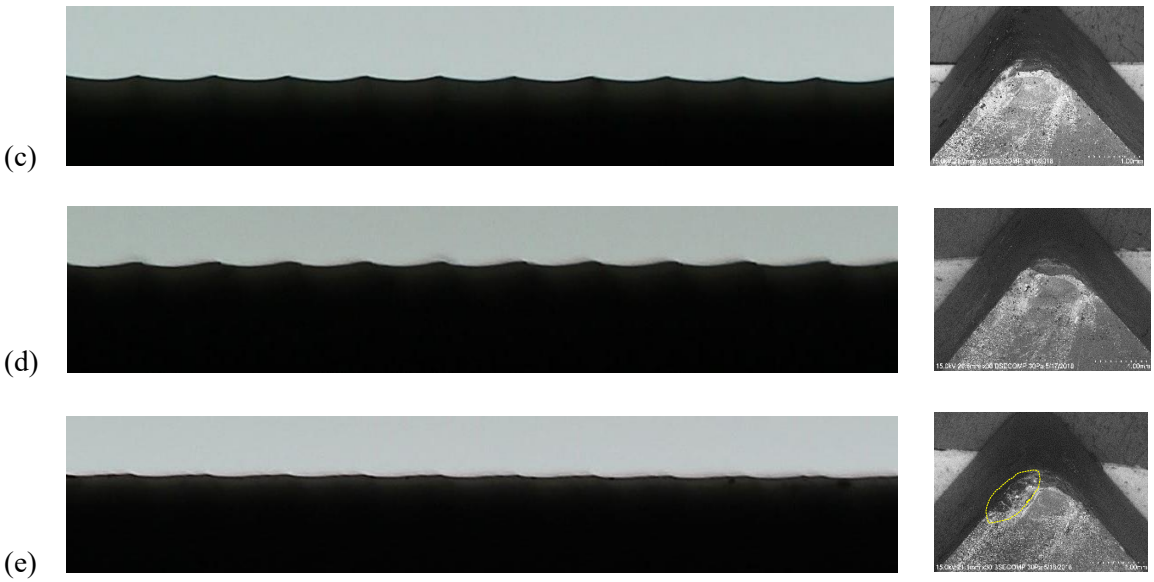

Figure 6. Workpiece edge profile and tool insert after (a) 1st pass, (b) 2nd pass, (c) 3rd pass, (d) 4th pass and (e) 5th pass.

In order to investigate the changes in profile in greater detail the length of profile equivalent to three feed spacing were cropped manually from the original image. Each image was rescaled to accommodate slight variation in the camera-to-workpiece distance after each machining pass. The cropped image was then subjected to sub-pixel edge location. The extracted edge profiles after the 2nd to the 5th passes were compared to the profile after the first pass. The extracted data were realigned so that the peaks in the subsequent passes match those in the first pass. Figures 7(a)-(l) shows the comparison between the 1st pass with subsequent passes at the start (Figures 7(a)-(d)), middle (Figures (7(e)-(h)) and end (Figures 7(i)-(l)). The start, middle sections of the workpiece are shown in Figure 1(b).

Comparison of the profiles shows that a significant change in the profile is visible after the 5th pass in all sections of the workpiece. This can be attributed to the significant loss of cutting tool material due to chipping as seen in insert image in Figure 6(e). Comparison of the changes in the profile between the 1st and subsequent passes at the various sections show that the middle and end sections of the workpiece produce very consistent results compared to the start section. The fluctuation in the profiles in the start section, especially after the 1st and 4th passes show the possible presence of vibration as the tool first comes in contact with the workpiece. As machining proceeds to the middle and end section the vibration effect has diminished and the changes in the workpiece profile due to tool wear and chipping becomes dominant.

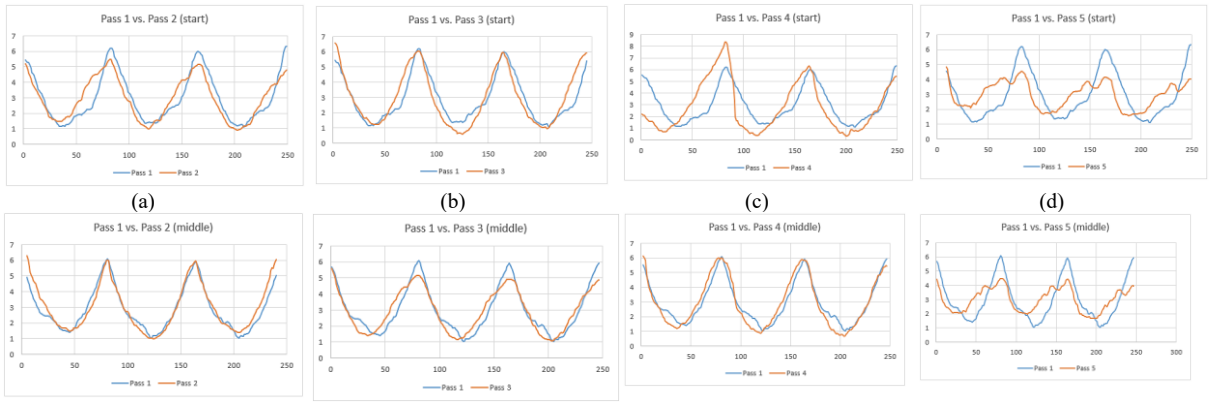

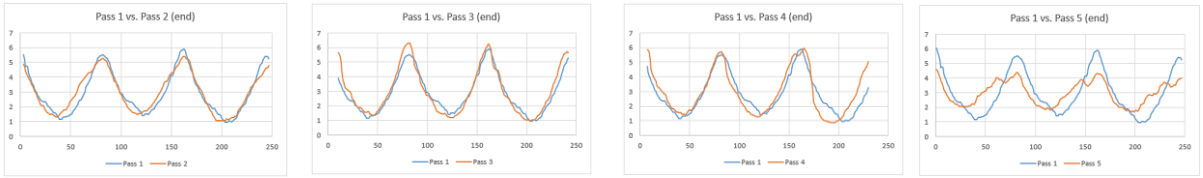

(i) (j) (k) (l)

Figure 7. (a)-(d) Comparison of surface profiles of workpiece between 1st and subsequent passes at: (a)-(d) start,(e)-(h) middle and (i)-(l) end of workpiece.

Figure 7 only shows a visual comparison of the profiles before and after tool chipping. In order to develop an automatic method of detecting chipping in the insert it is necessary to analyse the cross-correlation between these profiles. The maximum cross-correlation coefficients for the profiles are shown in Figure 8. Neglecting the data from the start section it can be seen that the maximum cross-correlation coefficient drops to below 0.8 after tool chipping. Thus, the correlation coefficient criteria for tool chipping can be set to 0.8 for the in-process detection of chipping in ceramic inserts.

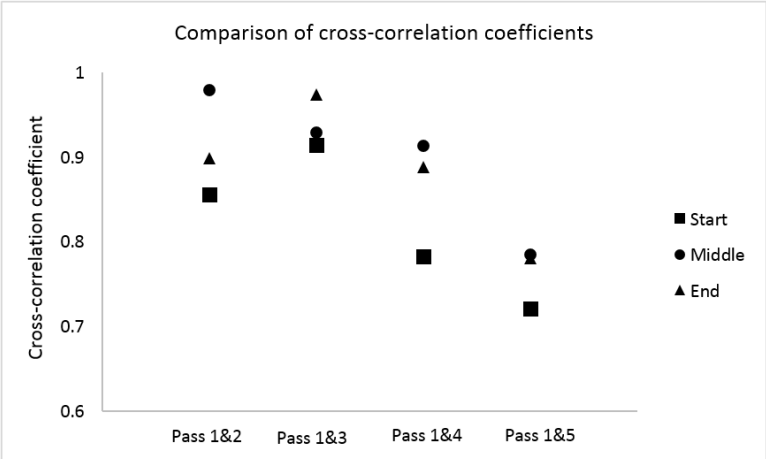

Figure 8. Comparison of cross-correlation coefficients for different machining passes.

4. Conclusion

A simple, yet effective, method of detecting chipping by analysis of the workpiece surface profile is proposed. Comparison of the surface profiles before and after chipping using cross-correlation shows a sharp decrease in the coefficient value after chipping. The study has also shown that the profiles compared should be extracted from the middle or end of each machining pass for better accuracy. The proposed method can be implemented for in-process tool chipping detection by capturing and processing the images in real-time during a turning process.

Acknowledgement

Part of this work was supported by the RU(I) grant (no. 1001/PMEKANIK/8014013). The authors would like to thank Universiti Sains Malaysia for the offer of the grant.

References

[1] Song J, Huang C, Lv M, Zou B, Liu H and Wang J 2014 Cutting performance and failure mechanisms of TiB_2-based ceramic cutting tools in machining hardened Cr12MoV mold steel *International Journal of Advanced Manufacturing Technology* 70 495-500

[2] Lima F F, Sales W F, Costa E S, da Silva F J and Machado A Á R 2017 Wear of ceramic tools when machining Inconel 751 using argon and oxygen as lubri-cooling atmospheres *Ceramics International* 43 (2017) 677–685
[3] Tan D-W, Guo W-M, Wang H-J, Lin H-T and Wang C-Y 2018 Cutting performance and wear mechanism of TiB_2-B_4C ceramic cutting tools in high speed turning of Ti6Al4V alloy *Ceramic International* (online 25 May 2018) In Press
[4] Mikołajczyk T, Nowicki K, Bustillo A and Yu Pimenov D 2018 Predicting tool life in turning operations using neural networks and image processing *Mechanical Systems and Signal Processing* 104 503-513
[5] Henrique L, Maia A, Abrao A M, Vasconcelos W L, Sales W F and Machado A R 2015 A new approach for detection of wear mechanisms and determination of tool life in turning using acoustic emission *Tribology International* 92 519-532
[6] Gutnichenko O, Bushlya V, Zhou J and Ståhl J-E 2017 Tool wear and machining dynamics when turning high chromium white cast iron with pcBN tools *Wear* 390-391 253-269
[7] Rmili W, Ouahabi A, Serra R, Leroy R 2016 An automatic system based on vibratory analysis for cutting tool wear monitoring *Measurement* 77 117-123
[8] Neslušan M, Mičieta B, Mičietová A, Čilliková M and Mrkvica I 2015 Detection of tool breakage during hard turning through acoustic emission at low removal rates *Measurement* 70 1-13
[9] Lee W K, Ratnam M M and Ahmad Z A 2016 Detection of fracture in ceramic cutting tools from workpiece profilesignature using image processing and fast Fourier transform *Precision Engineering* 44 131-142
[10] Lee W K, Ratnam M M and Ahmad Z A 2017 Detection of chipping in ceramic cutting inserts from workpiece profile during turning using fast Fourier transform (FFT) and continuous wavelet transform (CWT) *Precision Engineering* 47 406-423
[11] Lee W K, Ratnam M M and Ahmad Z A 2016 In-process detection of chipping in ceramic cutting tools during turning of difficult-to-cut material using vision-based approach *International Journal of Advanced Manufacturing Technology* 85 1275-1290
[12] Tabatabai A J and Mitchell OR 1984 Edge location to subpixel values in digital imagery *IEEE Transactions on Pattern Analysis and Machine Intelligence* 6(2) 188-201